J|A|C|S
ARTICLES
Published on Web 12/13/2001

Structure and Photophysics of an Old, New Molecule: 1,3,6,8-Tetraazatricyclo[4.4.1.1^{3,8}]dodecane

Jurriaan M. Zwier,[†] Albert M. Brouwer,[†] Wybren Jan Buma,*[,†] Alessandro Troisi,[‡] and Francesco Zerbetto*[,‡]

Contribution from the Institute of Molecular Chemistry, Faculty of Science, University of Amsterdam, Nieuwe Achtergracht 127-129, 1018 WS Amsterdam, The Netherlands, and Dipartimento di Chimica "G. Ciamician", Università degli Studi di Bologna, Via F. Selmi 2, 40126 Bologna, Italy

Received August 30, 2001

Abstract: More than a century after its initial synthesis, the static and dynamic geometry of 1,3,6,8-tetraazatricyclo [4.4.1.1^{3,8}]dodecane (TTD), a fully saturated cagelike molecule, is finally established. Detection and modeling of the supersonic jet fluorescence excitation and emission spectra show that the molecule undergoes interconversion between two S_4 symmetry minima. The barrier at the D_{2d} symmetric conformation is only 105 cm^{-1}, i.e., ~0.3 kcal mol^{-1}, and is overcome along a carbon−carbon torsional mode of a_2 symmetry. The presence of an S_4 conformation is corroborated by a Raman investigation. When excited to the first excited singlet state, the 3s Rydberg state, the molecule adopts a geometry with D_{2d} symmetry. The satisfactory description of the spectroscopy of TTD obtained by a combination of quantum chemical and quantum mechanical models is discussed, and the apparent conflict between the present results and nuclear magnetic resonance and X-ray diffraction experiments is solved. Because of the close analogy between a Rydberg state and the ground state of the radical cation regarding geometry and spectroscopic properties, it is concluded that the radical cation is also of D_{2d} symmetry.

I. Introduction

One of the success stories of theoretical organic chemistry is the understanding of the effects of vibro-electronic excitation in π-electron-conjugated systems. The qualitative picture that has emerged over the past 70 years is based on electron delocalization and shows that the excitation of molecules that alternate single and double bonds promotes binding electron density into antibonding orbitals and tends to elongate the formal double bonds and shorten the single bonds. This model has developed into such a high level of sophistication that prediction of Franck−Condon spectra is now quite accurate.[1] Recording and computational modeling of the electronic spectra of saturated systems is less common, possibly because of the lack of a simple conceptual framework similar to that used for π-systems. On one hand, the electron delocalization typical of conjugation is usually absent in these systems since the excitation promotes the electrons to an outer atomic orbital of the Rydberg type. On the other hand, it effectively creates radical-like species whose properties and chemistry are very different from those generated by π-excitations. High-symmetry, nonconjugated molecules can bridge the gap between conjugated molecules and saturated chromophores. In fact, symmetry-equivalent atoms must delocalize the excitation, while keeping the radicaloid nature of the wave function.

Molecules that form appealing bridges in this respect are saturated, cagelike amines, which have found application, for example, as electron donor groups in intramolecular electron donor−acceptor systems[2] and form part of natural products such as quinine. For their application as donor moieties, the internal reorganization energy upon oxidation is a crucial piece of information, since it partly determines the activation barrier for electron transfer. Over the past few years we have shown in several studies[3] that this internal reorganization energy can be well determined with high-resolution gas-phase spectroscopic studies of the lower-lying excited states of the neutral molecule

* To whom correspondence should be addressed. W.J.B.: fax +31-20-5256456, E-mail wybren@science.uva.nl. F.Z.: fax +39-051-2099456, E-mail gatto@ciam.unibo.it.
[†] University of Amsterdam.
[‡] Università degli Studi di Bologna.

(1) Zgierski, M. Z.; Zerbetto, F. *J. Chem. Phys.* **1993**, *98*, 14. Zerbetto, F.; Zgierski, M. Z. *J. Chem. Phys.* **1993**, *98*, 4822. Zgierski, M. Z.; Zerbetto, F. *J. Chem. Phys.* **1993**, *99*, 3721. Orlandi, G.; Palmieri, P.; Tarroni, R.; Zerbetto, F.; Zgierski, M. Z. *J. Chem. Phys.* **1994**, *100*, 2458. Zerbetto, F.; Zgierski, M. Z. *J. Chem. Phys.* **1994**, *101*, 1842. Zerbetto, F. *J. Am. Chem. Soc.* **1995**, *117*, 1621. Zerbetto, F. *J. Phys. Chem.* **1994**, *98*, 13157. Zerbetto, F. *Chem. Phys. Lett.* **1995**, *241*, 445. Buma, W. J.; Zerbetto, F. *J. Chem. Phys.* **1995**, *103*, 10492. Buma, W. J.; Zerbetto, F. *J. Am. Chem. Soc.* **1996**, *118*, 9178. Buma, W. J.; Zerbetto, F. *J. Phys. Chem. A* **1999**, *103*, 2220.
(2) Dekkers, A. W. J. D.; Verhoeven, J. W.; Speckamp, W. N. *Tetrahedron* **1973**, *29*, 1691. Worell, C.; Verhoeven, J. W.; Speckamp, W. N. *Tetrahedron* **1974**, *30*, 3525. Wiering, P. G.; Verhoeven, J. W. *Recl. Trav. Chim. Pays-Bas* **1996**, *115*, 303. Philips, D. L.; Gould, I. R.; Verhoeven, J. W.; Tittelbach-Helmrich, D.; Myers, A. B. *Chem. Phys. Lett.* **1996**, *258*, 87. Lilichenko, M.; Verhoeven, J. W.; Myers, A. B. *Spectrochim. Acta A* **1997**, *53*, 2079. Lilichenko, M.; Tittelbach-Helmrich, D.; Verhoeven, J. W.; Gould, I. R.; Myers, A. B. *J. Chem. Phys.* **1998**, *109*, 10958. Eckhardt, W.; Grob, C. A.; Treffert, W. D. *Helv. Chim. Acta* **1972**, *55*, 2432. Eckhardt, W.; Grob, C. A.; Treffert, W. D. *Tetrahedron Lett.* **1973**, *37*, 3627.
(3) Zwier, J. M.; Wiering, P. G.; Brouwer, A. M.; Bebelaar, D.; Buma, W. J. *J. Am. Chem. Soc.* **1997**, *47*, 11523. Zwier, J. M.; Brouwer, A. M.; Rijkenberg, A.; Buma, W. J. *J. Phys. Chem. B* **2000**, *104*, 729. Balakrishnan, G.; Keszthelyi, T.; Wilbrandt, R.; Zwier, J. M.; Brouwer, A. M.; Buma, W. J. *J. Phys. Chem. B* **2000**, *104*, 1834.

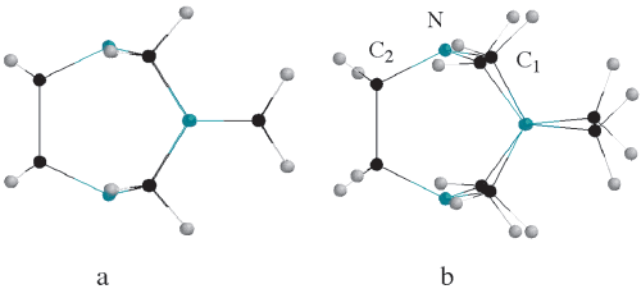

Figure 1. Eclipsed (D_{2d}) conformation (a) and gauche (S_4) conformation (b) of TTD.

in combination with ab initio calculations of the equilibrium geometry and force field of the ground state of the neutral and radical cationic forms of the molecule, and the concept that the geometrical and vibrational properties of the lower excited Rydberg singlet states resemble to a large extent those of the ground state of the radical cation.

The subject of the present study is the compound 1,3,6,8-tetraazatricyclo[4.4.1.1^{3,8}]dodecane, $C_8H_{16}N_4$ (TTD). In its most symmetric conformation (Figure 1a), the molecule has only five symmetry nonequivalent atoms (one nitrogen, two carbons, and two hydrogens). The lower excited states derive from the excitation from an orbital that is formed by a linear combination of the four nitrogen lone pair orbitals to final orbitals in the $n = 3$ shell that are linear combinations of Rydberg atomic orbitals. The cage structure of the molecule brings carbon and nitrogen atoms close, so that the effect of the excitation may effectively be delocalized in a way similar to that of conjugated systems. A celebrated example of another cage structure with delocalized excitations is Buckminsterfullerene, or C_{60}, whose π molecular orbitals have been assessed, modeled, and rationalized in terms of the spherical harmonics that is the angular component of the atomic orbitals of the most symmetric chemical object, viz., the hydrogen atom.[4] The fundamental question that arises concerns the generality of the correspondence of the electronic systems of cage molecules with the hydrogen-atom-like orbitals.

Apart from this more physical angle, the molecule is also of interest from various chemical points of view. After the discovery of the remarkable stability of the radical cation of 1,4-diazabicyclo[2.2.2]octane (DABCO) by McKinney and Geske,[5] several alkylamines were studied using cyclic voltammetry (CV).[6] DABCO shows a re-reduction wave in the CV experiment, and an ESR signal of the radical cation can be observed at room temperature. Most other alkylamines show irreversible waves because decomposition of the radical cation occurs rapidly.[7] TTD, containing two N−C−C−N DABCO-like linkages, is one of the tertiary alkylamines that also show a re-reduction wave. Later, Alder et al.[8] showed that radical cations containing 1,5-diazabicyclo[3.3.3]undecane units are even more stable than DABCO$^+$, but these have through-space rather than through-bond overlap of the nitrogen lone pairs, which leads to a two-center, three-electron σ bond.

The structure of TTD has long been elusive. It was first synthesized in 1898 by condensation of 1,2-diaminoethane with formaldehyde,[9] but originally its structure was believed to be 1,3,6,8-tetraazatricyclo[6.2.1.1^{3,6}]dodecane. Only after measurement of its ^{1}H NMR spectrum,[10] which showed two different types of hydrogens, the 1,3,6,8-tetraazatricyclo [4.4.1.1^{3,8}]-dodecane structure was confirmed. The subsequent determination of the crystal structure[11] indeed agreed with the ^{1}H NMR assignment. While by now the structure of the neutral molecule would seem well established, the structure of the radical cation is still unclear. ESR splittings for the four nitrogen atoms were found to be 7.09 G, whereas two hydrogen splittings of 7.68 and 4.14 G, respectively, were found.[12] These values could not be rationalized using a D_{2d}-symmetric structure. A proposed C_{2v} structure, in which the charge would be localized on two nitrogen atoms, gave predicted ESR splittings far off from the experimental values as well. This led to several suggestions, including an inversion of orbital symmetry upon ionization, but no conclusive evidence for the structure of the radical cation could be found (see, however, section III).

In the present work, a combination of experimental and computational techniques is used to investigate the nature of the ground state of the neutral molecule and that of the radical cation, as well as to assess the effect of electronic excitation in TTD. It will be shown that these studies lead to the unambiguous conclusion that the conformation of lowest energy in the ground state is not of D_{2d} but S_4 symmetry, and that the symmetry of the excited Rydberg states—and implicitly also that of the ground state of the radical cation—is D_{2d}. A thorough understanding of the vibrationally resolved spectra of the molecule will allow the discussion of the structure−photophysics relationship in a wider context that includes the origin of the drive to lower its symmetry in the ground state with respect to the higher symmetry observed in the first electronically excited state.

II. Experimental and Theoretical Details

A. Experimental Procedures. The experimental setup for performing fluorescence excitation and single-level emission spectroscopy on TTD has been described in detail in refs 3 and 13. For the supersonic jet experiments on TTD, a 0.5 mm pulsed valve (General Valve Iota One System) was used that was synchronized with the XeCl excimer laser working at a repetition rate of 38 Hz, and pumping a dye laser operating on Coumarine 540. To obtain a sufficiently high vapor pressure, the temperature of the sample reservoir was set at 60 °C for the excitation as well as the fluorescence measurements. In the fluorescence excitation experiments, a monochromator was used at a center wavelength of 320 nm and with a slit width of 3 mm, resulting in a spectral resolution of 7.5 nm. The $S_1 \leftarrow S_0$ excitation spectrum was obtained by scanning the dye laser in steps of 0.05 cm^{-1} and averaging the signal over 60 laser pulses per step. The fluorescence signal was divided by the laser intensity as measured by a radiometer. Single-level emission spectra were obtained with a slit width of 0.05 mm, resulting in a resolution of about 10 cm^{-1}, and averaging the signal over 75 laser pulses. In these experiments, the photomultiplier was cooled (−78 °C) with a mixture of ethanol and dry ice to reduce the dark current.

(4) Dresselhaus, M. S.; Dresselhaus, G.; Eklund, P. C. *Science of Fullerenes and Carbon Nanotubes*; Academic Press: San Diego, CA, 1996. Savina, M. R.; Lohr, L. L.; Francis, A. H. *Chem. Phys. Lett.* **1993**, *205*, 200.
(5) McKinney, T. M.; Geske, D. H. *J. Am. Chem. Soc.* **1965**, *87*, 3013.
(6) Nelsen, S. F.; Hintz, P. J. *J. Am. Chem. Soc.* **1972**, *94*, 7114.
(7) Lindsay-Smith, J. R.; Masheder, D. *J. Chem. Soc., Perkin Trans. 2* **1977**, 1732.
(8) Alder, R. W.; Arrowsmith, R. J.; Casson, A.; Sessions, R. B.; Heilbronner, E.; Kovac, B.; Huber, H.; Taagepera, M. *J. Am. Chem. Soc.* **1981**, *103*, 6137. Alder, R. W. *Tetrahedron* **1990**, *46*, 683.
(9) Bischoff, C. A. *Chem. Ber.* **1898**, *31*, 3248.
(10) Volpp, G. *Chem. Ber.* **1962**, *95*, 1493.
(11) Murray-Rust, P. *J. Chem. Soc., Perkin Trans. 2* **1974**, 1136.
(12) Nelsen, S. F.; Buschek, J. M. *J. Am. Chem. Soc.* **1974**, *96*, 6424.
(13) Rijkenberg, R. A.; Bebelaar, D.; Buma, W. J. *J. Am. Chem. Soc.* **2000**, *122*, 7418.

Table 1. Selected Calculated and Experimental Geometrical Parameters (Å and Degrees) of TTD Ground State (For the Atom Numbering See Figure 1)

	exptl[a]	HF (D_{2d})	HF (S_4)	MP2 (D_{2d})	MP2 (S_4)	B3LYP (D_{2d})	B3LYP (S_4)
$N-C_1$	1.470(7)	1.450	1.451	1.459	1.459	1.464	1.464
$N-C_{1'}$	1.470(7)	1.450	1.450	1.459	1.461	1.464	1.465
$N-C_2$	1.450(7)	1.448	1.449	1.455	1.456	1.458	1.458
$C_2-C_{2'}$	1.534(8)	1.556	1.555	1.559	1.550	1.570	1.570
C_1-H_1	0.98(3)	1.085	1.085	1.098	1.098	1.097	1.097
$C_1-H_{1'}$	0.98(3)	1.085	1.084	1.098	1.097	1.097	1.097
C_2-H_2	1.09(3)	1.085	1.085	1.097	1.096	1.097	1.097
$C_2-H_{2'}$	1.09(3)	1.085	1.086	1.097	1.099	1.097	1.098
$N-N'$	2.90	2.785	2.785	2.820	2.823	2.825	2.826
NC_1N	116.9(3)	117.9	117.9	118.9	118.7	118.6	118.6
$NC_2C_{2'}$	118.9(2)	115.1	115.0	115.7	115.1	115.5	155.5
$C_1NC_{1'}$	119.3(3)	115.3	115.2	114.9	114.8	115.0	115.0
C_1NC_2	111.9(2)	115.1	115.1	114.7	114.2	114.9	114.8
$C_{1'}NC_2$	111.9(2)	115.1	115.1	114.7	114.5	114.9	114.9
$\sum N$[b]	343.1	345.5	345.4	344.3	343.5	344.7	344.7
$N-C_2-C_{2'}-N'$	0	0	6.3	0	20.3	0	1.2

[a] X-ray data from ref 11. [b] An indicator for the hybridization around the nitrogen ($2 \times C_1NC_2 + C_1NC_{1'}$).

The FT-Raman spectrum with a resolution of 4 cm^{-1} has been obtained using a Bruker RFS 100 employing a Nd:YAG laser giving 400 mW at 1064 nm.

TTD was obtained as a gift from Prof. Stephen F. Nelsen.[9]

B. Theoretical Procedures. Ab initio calculations on the ground state of the neutral molecule and of the radical cation of TTD were performed using the Gaussian suite of programs.[14] Optimized geometries and harmonic force fields were obtained using Hartree−Fock or the hybrid density functional (U)B3LYP[15] methods with the 6-31G* basis set.[16] For the ground state of the neutral molecule, calculations have also been performed at the MP2 level. For the excited state, the optimized geometry and the harmonic force field were obtained using Configuration Interaction Singles (CIS) with the 6-31+G* basis set.

III. Results and Discussion

In its most symmetric conformation, TTD belongs to the D_{2d} point group (Figure 1a). Chemical considerations based on the hydrogen−hydrogen interaction in the $N-CH_2-CH_2-N$ fragments suggest that twisting about the C−C bond could lower the energy of the molecule and transform it to S_4 symmetry (Figure 1b). The lower strain of the pseudo-gauche conformation of the CH_2-CH_2 groups would not be at odds with the NMR analysis[10] if the interconversion between the two equivalent S_4 conformers through the intermediate D_{2d} geometry were rapid on the NMR time scale. The crystal structure analysis[11] may also be consistent with the lower symmetry, for instance, if the interconversion barrier is sufficiently low that the crystal packing forces can overcome it. Another explanation will be discussed below.

Optimization of the geometry at the HF level within D_{2d} constraints leads to a structure whose harmonic force field gives rise to an imaginary frequency of 31 cm^{-1}. Further optimization after distortion along the associated normal mode results in a stable S_4 minimum with an $N-CH_2-CH_2-N$ torsion angle of 6.3°, but with essentially the same energy as the D_{2d} structure. Geometry optimization at the B3LYP/6-31G* level, on the other hand, leads to a D_{2d} structure that proved to be a minimum on the potential energy surface. An S_4 minimum, only 0.1 kcal/mol lower in energy than the D_{2d} structure, was also found, although the associated geometry turns out to be very close to the D_{2d}-symmetric structure. The only difference is the $N-CH_2-CH_2-N$ torsional angle, which is 1.2° instead of 0° for the D_{2d} conformation. HF/MP2 calculations, finally, in contrast with the other computational models, predict a clear S_4 minimum with an $N-CH_2-CH_2-N$ torsion angle of 20° and an energy lowering of 0.32 kcal mol^{-1} with respect to the D_{2d} structure. The different methods thus agree on the existence of a minimum in the S_4 symmetry but leave some uncertainty about the displacement of the S_4 structure from the D_{2d} symmetry and the height of the energy barrier that connects the two conformers.

A summary of the most relevant results of the quantum chemically optimized structural parameters is reported in Table 1 for both the S_4 and D_{2d} structures. A feature of interest is the rather flat nitrogen environment in the ground state, indicated by the high value of the sum of the bond angles around the nitrogen ($\sum N$). This is caused by the fused seven-membered rings. The values of the structural parameters calculated with the different methods are all rather similar, and the differences between the D_{2d} and S_4 structures are small. Only the $N-CH_2-CH_2-N$ torsional angle differs substantially.

The ground-state Raman spectrum has been measured in the solid (Figure 2). The assignments reported in Table 2 have been guided by the calculated B3LYP/6-31G* frequencies of the D_{2d} B3LYP/6-31G* structure and by the MP2/6-31G* frequencies of the S_4 MP2/6-31G* structure. In some cases the Raman intensity calculations at the HF/6-31G* level have been taken into account to come to an unambiguous assignment. There are differences up to 25 cm^{-1} between the frequencies calculated for the D_{2d} and S_4 structures, but this does not influence the assignments. What is rather important is the transition observed

(14) Frisch, M. J.; Trucks, G. W.; Schlegel, H. B.; Scuseria, G. E.; Robb, M. A.; Cheeseman, J. R.; Zakrzewski, V. G.; Montgomery, J. A., Jr.; Stratmann, R. E.; Burant, J. C.; Dapprich, S.; Millam, J. M.; Daniels, A. D.; Kudin, K. N.; Strain, M. C.; Farkas, O.; Tomasi, J.; Barone, V.; Cossi, M.; Cammi, R.; Mennucci, B.; Pomelli, C.; Adamo, C.; Clifford, S.; Ochterski, J.; Petersson, G. A.; Ayala, P. Y.; Cui, Q.; Morokuma, K.; Malick, D. K.; Rabuck, A. D.; Raghavachari, K.; Foresman, J. B.; Cioslowski, J.; Ortiz, J. V.; Stefanov, B. B.; Liu, G.; Liashenko, A.; Piskorz, P.; Komaromi, I.; Gomperts, R.; Martin, R. L.; Fox, D. J.; Keith, T.; Al-Laham, M. A.; Peng, C. Y.; Nanayakkara, A.; Gonzalez, C.; Challacombe, M.; Gill, P. M. W.; Johnson, B. G.; Chen, W.; Wong, M. W.; Andres, J. L.; Head-Gordon, M.; Replogle, E. S.; Pople, J. A. *Gaussian 98*, revision A.5; Gaussian, Inc.: Pittsburgh, PA, 1998.
(15) Becke, A. M. *J. Chem. Phys.* **1993**, *98*, 5648.
(16) Foresman, J. B.; Head-Gordon, M.; Pople, J. A.; Frisch, M. J. *J. Chem. Phys.* **1992**, *96*, 135. Frisch, M. J.; Pople, J. A.; Binkley, J. S. *J. Chem. Phys.* **1984**, *80*, 3265.

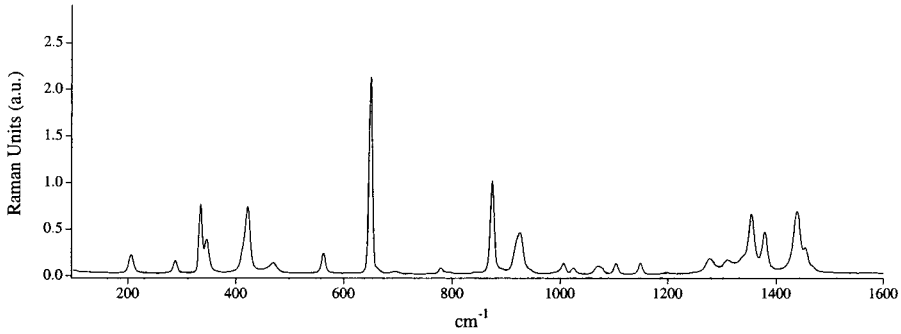

Figure 2. Ground-state FT-Raman spectrum of TTD (150−1600 cm^{-1}).

Table 2. Experimental (FT Raman) Frequencies (cm^{-1}) and Intensities Together with the Calculated Fundamental Vibrational Wavenumbers (cm^{-1}) of TTD in the Ground State (D_{2d} and S_4)

					relative intensity						relative intensity
		MP2[c] (D_{2d})	MP2[b] (S_4)	exptl[c]	(exptl)			MP2[c] (D_{2d})	MP2[b] (S_4)	exptl[c]	(exptl)
a_1[a]	ν_{11}	318	314	334	0.73	b_1[a]	ν_{29}	194	196	206	0.19
(a)	ν_{10}	630	631	649	2.10	(b)	ν_{28}	390	391	422[g]	0.70
	ν_9	855	854	874	0.98		ν_{27}	983	990		
	ν_8	908	914				ν_{26}	1137	1137	1149[g]	0.10
	ν_7	1116	1110	1104	0.10		ν_{25}	1224	1223		
	ν_6	1314	1314	1354	0.66		ν_{24}	1314	1289	1310[j]	0.14
	ν_5	1373	1368	1379[d]	0.44		ν_{23}	1434	1440	1439[e]	0.66
	ν_4	1439	1443	1439[e]	0.66		ν_{22}	2897	2901		
	ν_3	1474	1477				ν_{21}	2951	2951		
	ν_2	2901	2902			b_2	ν_{40}	328	324	345	0.36
	ν_1	2918	2914			(b)	ν_{39}	432	451	469	
a_2	ν_{20}	i66	96				ν_{38}	774	774	779[h]	0.05
(a)	ν_{19}	449	445	469	0.11		ν_{37}	908	910	925[k]	0.43
	ν_{18}	924	927				ν_{36}	1017	1019	1025	0.05
	ν_{17}	980	983				ν_{35}	1279	1269	1278	0.15
	ν_{16}	1179	1183	1197[f]	0.01		ν_{34}	1317	1338		
	ν_{15}	1270	1254				ν_{33}	1363	1361	1379[d]	0.44
	ν_{14}	1334	1340				ν_{32}	1468	1469		
	ν_{13}	2948	2950				ν_{31}	2914	2908		
	ν_{12}	2957	2959				ν_{30}	2958	2962		
d	ν_{59}	264	263	288	0.13	*d*	ν_{49}	1323	1322		
(e)	ν_{58}	403	407	422[g]	0.70	(e)	ν_{48}	1339	1346		
	ν_{57}	548	545	563	0.21		ν_{47}	1355	1354	1379[d]	0.44
	ν_{56}	631	625				ν_{46}	1436	1442	1439[e]	0.66
	ν_{55}	771	768	779[h]	0.05		ν_{45}	1457	1462	1454	0.27
	ν_{54}	860	868				ν_{44}	2898	2900		
	ν_{53}	989	989	1007[i]	0.10		ν_{43}	2908	2905		
	ν_{52}	1083	1075	1070	0.07		ν_{42}	2955	2957		
	ν_{51}	1136	1131	1149[g]	0.10		ν_{41}	2973	2973		
	ν_{50}	1291	1286								

[a] Normal mode symmetry in D_{2d} (S_4 in parentheses). [b] MP2/6-31G* (scaling factor 0.9427). [c] FT-Raman data with a resolution of 4 cm^{-1}. [d] This band can be assigned to an a_1 or to a b_2 vibration. [e] This band can be assigned to an a_1 or to an e vibration. [f] These vibrations can only be assigned to a_2 vibrations, although these are not allowed Raman transitions in D_{2d}. This is in agreement with the S_4 symmetry of the molecule. [g] This band can be assigned to an e or to a b_1 vibration. [h] This band can be assigned to an e or to a b_2 vibration. [i] This band is assigned to ν_{53}, because ν_{27} has a negligible intensity according to HF/6-31G* calculations. [j] This band is assigned to ν_{24}, because ν_{50} has a negligible intensity according to HF/6-31G* calculations. [k] This band is assigned to ν_{37}, because ν_8 has a negligible intensity according to HF/6-31G* calculations.

at 1197 cm^{-1}. This band does not derive from the transition to one of the Raman-allowed fundamental transitions. Similarly, it is found that an assignment in terms of a combination band runs into problems on account of the intensities of the associated fundamental transtions. Careful analysis suggests that it might be assigned to mode ν_{16} of a_2 symmetry for the D_{2d} structure, but we hasten to notice that the low intensity of the band precludes any definite and unambiguous assignment. Since a_2 vibrations are not Raman allowed in D_{2d}, its appearance must be due to a lowering of the symmetry in the ground state. Indeed, in the S_4 point group ν_{16} would be of a symmetry and would be allowed in Raman spectroscopy. The Raman measurements would therefore be in contradiction with the high symmetry originally deduced from the NMR and crystal structure analyses.

To settle conclusively the question of whether TTD in its electronic ground state is of D_{2d} symmetry or not, and to determine as well the geometry of the molecule in the ground state of its radical cation, we have studied the first excited singlet state—the 1^1B_2 state of 3s Rydberg character—with fluorescence excitation and dispersed emission spectroscopy under supersonic jet expansion conditions. Figure 3 shows as a prelude to these studies the electronic absorption spectrum of TTD in *n*-hexane solution. Surprisingly, electronic spectroscopy studies of TTD have so far not been reported. The spectrum shows a gradual

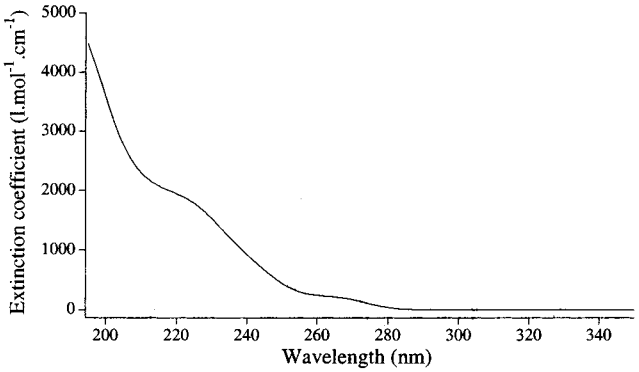

Figure 3. Electronic absorption spectrum of TTD in *n*-hexane.

increase of absorbance from 280 nm to smaller wavelengths. The long-wavelength transition is at a relatively low energy compared to those of other trialkylamines but is similar to that for 1,4-diazabicyclo[2.2.2]octane.[17] The first absorption band, with an origin at 285.74 nm in the gas phase (vide infra), is due to a transition from the 1^1A_1 electronic ground state to the 1^1B_2 state of 3s Rydberg character, a one-photon transition that is symmetry allowed in the D_{2d} point group. The second transition to the excited state of ^1E symmetry with $3p_{x,y}$ Rydberg character has its origin at 255.8 nm in the gas phase.[18]

The fluorescence excitation spectrum of the $S_1 \leftarrow S_0$ transition of TTD seeded in a 3 bar He expansion is shown in Figure 4. Assignments of the major bands in this spectrum are reported in Table 3. The most remarkable feature of the spectrum is the apparent progression based on the 0−0 transition and on all the other fundamental vibrations. This progression is remarkable for two reasons. First, Table 2 shows that the progression cannot be associated with a totally symmetric vibration since the lowest vibrational frequency of a totally symmetric vibration is expected around 300 cm^{-1}. Second, the spacing between the bands is rather irregular, and the observed intensity pattern defies every normal expectation. Further clues as to how to interpret these observations are obtained by considering the dispersed emission spectra measured for the 0−0 transition and seven members of the vibronic progression (Figure 5). In these spectra, a progression similar to that seen in excitation is visible; members of this progression are marked with an asterisk. Comparison of the spectra in Figure 5a, c, e, and g, obtained after excitation to the first, third, fifth, and seventh bands of the progression (odd series), with those in Figure 5b, d, f, and h, obtained after excitation to the second, fourth, sixth, and eighth bands of the progression (even series), shows that they differ considerably in the spacings between the members of the indicated progression. In particular, the odd series starts with a spacing of 64 cm^{-1}, while the even series begins with 85 cm^{-1}. We also notice that, with respect to the intensity distribution over the bands of the progression, the spectra seem to come in pairs: Figure 5a resembles Figure 5b, Figure 5c resembles Figure 5d, etc. This analysis thus indicates that the progression observed in the excitation spectrum must be considered as consisting of two parts. The first part, starting with the 0−0 transition, is characterized by spacings from 155.7 up to 168.7, 182.5, 193.3, and 205.1 cm^{-1}. The second progression starts at the resonance

Table 3. Assignment of the Major Bands of the $S_1 \leftarrow S_0$ Fluorescence Excitation Spectrum of TTD

excitation band	intensity[a]	assignment[b]	excitation band	intensity[a]	assignment[b]
0.0	100.0	origin	953.1	11.9	
2.0	6.4		959.4	16.1	
74.5	121.9	20_0^1	962.3	42.4	
76.3	11.1	20_0^1 + 1.8	964.6	30.4	$20_0^1 8_0^1$
155.7	199.6	20_0^2	965.4	21.8	
157.2	30.2	20_0^2 + 1.5	971.6	27.3	$20_0^4 10_0^1$
237.0	158.0	20_0^3	1039.9	15.7	
324.4	202.8	20_0^4	1040.5	36.3	
350.4	16.0	11_0^1	1045.1	75.9	$20_0^2 8_0^1$
412.7	97.2	20_0^5	1059.6	15.0	
424.5	17.4	$20_0^1 11_0^1$	1080.8	20.1	7_0^1
505.2	15.5	$20_0^2 11_0^1$	1122.3	35.2	
506.9	100.9	20_0^6	1125.9	25.0	$20_0^3 8_0^1$
586.1	20.6	$20_0^3 11_0^1$	1131.4	14.4	
600.7	32.2	20_0^7	1134.5	33.5	
644.9	17.8	10_0^1	1153.6	15.5	
673.1	25.6	$20_0^4 11_0^1$	1156.4	19.1	$20_0^1 7_0^1$
700.2	18.5	20_0^8	1209.4	42.3	
719.9	23.6	$20_0^1 10_0^1$	1216.5	32.5	
720.3	15.2		1222.5	15.5	
761.0	10.8	$20_0^5 11_0^1$	1237.2	30.2	$20_0^2 7_0^1$
801.1	55.2	$20_0^2 10_0^1$	1299.9	13.3	
855.1	11.6	$20_0^6 11_0^1$	1304.6	31.1	
879.2	24.7		1319.1	14.0	$20_0^3 7_0^1$
883.8	25.0	$20_0^3 10_0^1$	1320.6	16.1	
890.1	35.0	8_0^1[c]	1394.8	24.7	$20_0^4 7_0^1$
905.3	3.8	20_0^{10}	1398.4	20.1	

[a] Relative to the intensity of the origin. [b] For normal mode assignment, see Table 2. [c] Ambiguous.

74.5 cm^{-1} displaced from the 0−0 transition and has spacings of 162.5, 175.7, and 188 cm^{-1}. A final piece of important information is obtained when excitation spectra at different distances from the nozzle, i.e., at different temperatures, are considered. An example is given in Figure 6 for the first two bands of the progression. This figure shows that the ratio of the intensities of these two bands is dependent on the temperature at which the molecule is probed. Such a behavior can be explained only if two "species" are populated in the ground state. The observed temperature dependence and experimental conditions indicate at the same time, however, that the energy difference between these two species is only on the order of some calories per mole.

With the calculations and the measured Raman spectrum in mind, it is concluded that the following model must apply. In the ground state, the potential energy surface along the ν_{20} mode of a_2 symmetry in D_{2d} symmetry, i.e., the torsional mode along the N−CH_2−CH_2−N dihedral angle that lowers the symmetry of the molecule to S_4, forms a double minimum potential. The barrier is, however, sufficiently low to give +/− levels separated by the so-called tunneling splitting. The pattern of vibrational levels is shown in Figure 7. At the bottom of the well, the splitting is small. The levels of the second torsional quantum are just below the top of the barrier, and the splitting between them increases to ∼21 cm^{-1}. At higher energy, the potential becomes more similar to that of a harmonic oscillator, and its levels deviate less from harmonicity. The even-numbered ground-state vibrational levels, ψ_+, have an effective A_1 symmetry, while

(17) Robin, M. B. *Higher Excited States of Polyatomic Molecules*; Academic Press: New York, 1974; Vol. 1.
(18) Zwier, J. M. Thesis, University of Amsterdam, 2000.

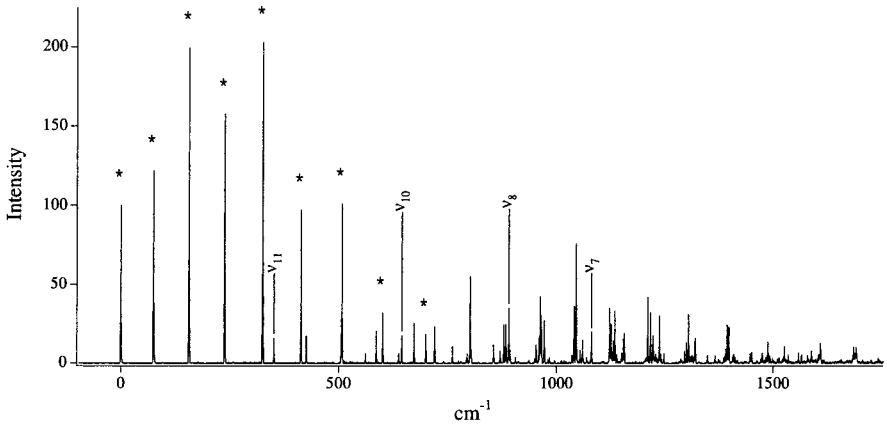

Figure 4. Fluorescence excitation spectrum of the $S_1 \leftarrow S_0$ transition of TTD. The excitation energy is given with respect to the energy of the 0−0 transition located at 34997 cm^{-1}. Transitions to the fundamentals of a_1 vibrations are marked. The bands denoted with an asterisk are part of a progression of the ν_{20} (a_2 in D_{2d} symmetry) torsional mode on the 0−0 transition (see text). Assignments of the major bands up to 1400 cm^{-1} above the 0−0 transition are given in Table 3.

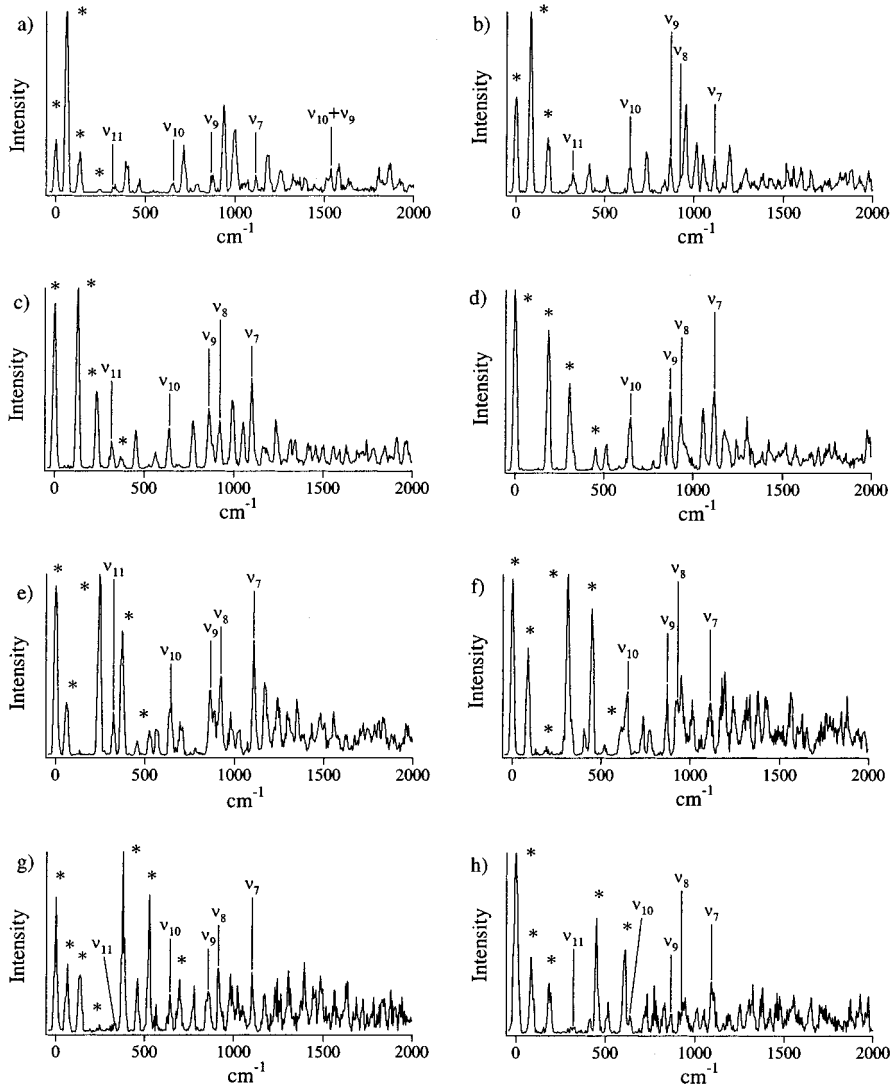

Figure 5. Single-level dispersed emission spectra from selected levels of S_1 of TTD. Excitation occurs in (a) via the 0−0 transition, in (b)−(h) via the bands 74.5 cm^{-1} (b), 155.7 cm^{-1} (c), 237.0 cm^{-1} (d), 324.4 cm^{-1} (e), 412.7 cm^{-1} (f), 506.9 cm^{-1} (g), 600.7 cm^{-1} (h) displaced from the 0−0 transition.

the odd-numbered levels, ψ_-, belong to A_2 symmetry. In S_1, the levels of the torsional coordinate behave as quasi-harmonic, see Figure 8. Since the irreducible representation of S_1 is B_2, an even number of $\nu_{20}(a_2)$ quanta give vibronic levels of B_2 symmetry, while an odd number of ν_{20} quanta give vibronic levels of B_1 symmetry. One-photon transitions occur either

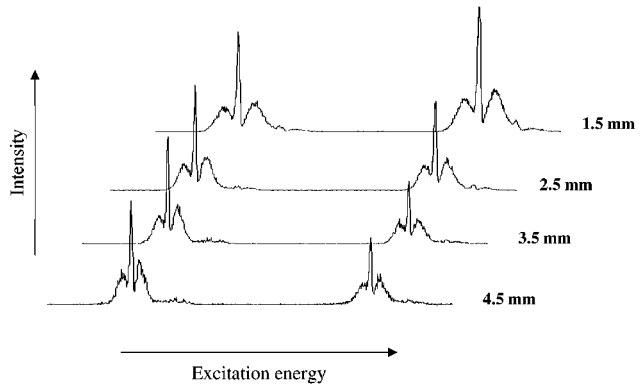

Figure 6. Dependence of the intensities of the 0−0 transition (left) and the transition 74.5 cm^{-1} displaced to higher energies (right) on probe conditions. Indicated are the distances from the nozzle where excitation occurs.

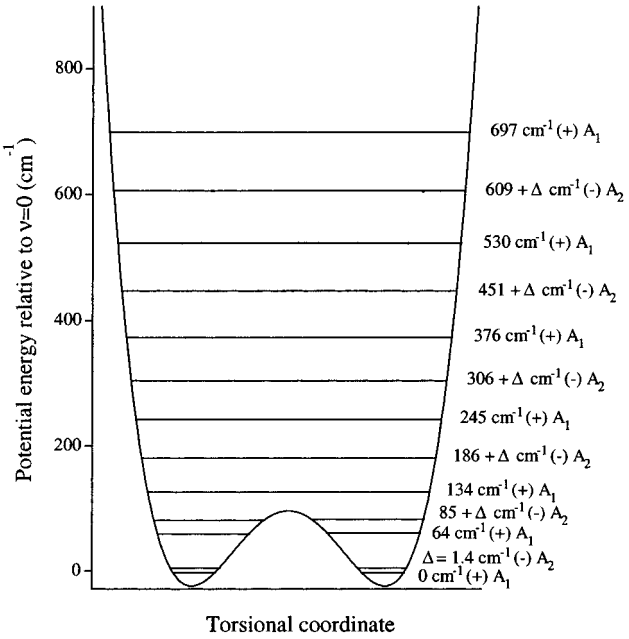

Figure 7. Energy levels and potential energy function of the ν_{20} torsional vibration in the ground state as deduced from the fluorescence excitation and emission spectra. The vibrational levels are given with their symmetry and parity. Δ is the tunneling splitting of the first torsional quantum; its value results from the fitting of the experimental data to a quantum mechanical model (see text).

via the *z*-component of the dipole operator, which is of B_2 symmetry, or via the (*x*,*y*) component, which is of E symmetry. For the $S_1 \leftrightarrow S_0$ transitions, this implies that transitions between the electronic ground-state levels of A_1 symmetry and the excited-state B_2 levels are allowed, and transitions between the electronic ground-state levels of A_2 symmetry and the excited-state B_1 levels are allowed. The pattern of alternating symmetry levels governs the intensity and spacing of the spectra. Fitting the levels of the excited state observed in the excitation spectrum to the vibrational energies of an anharmonic oscillator (vide infra) leads to a tunneling splitting, Δ, of 1.4 cm^{-1}. This number is in good agreement with our conclusion from Figure 6 that the energy difference between the two "species"—now identified as being the two tunneling-splitted components of first torsional quantum—is rather small.

The observed excitation and emission spectra allow for a reconstruction of the potential energy surfaces of ν_{20} in the ground and first excited states. For this purpose we express the $\nu_{20}(a_2)$ potential energy curve in terms of an expansion over even powers of the coordinate. Odd terms would produce minima of different energy and are absent by symmetry. The simplest choice is to retain only the quadratic and the quartic terms. A double minimum can be formed for a certain range of coefficients of the two terms whose coefficients, for simplicity, are called *a* for the quadratic term and *b* for the quartic term. The use of a quadratic−quartic potential was introduced by Bell[19] in the study of ring-puckering problems. Other possible choices[20] have shown to be essentially equivalent.[21] Inclusion of higher terms is straightforward, although unnecessary in this case. The mass of the vibration, *m*, is taken as 1.800 atomic mass units from the MP2 calculations. Variation of *m* upon changing the computational model (B3LYP, HF) is within 1%. Following previous work,[22] numerical solutions are obtained on the basis of the harmonic oscillator functions. About 200 basis functions are needed to ensure full convergence of the lowest 12 energy levels. Fitting of the vibrational levels observed in the spectroscopic experiments then leads to the parameters reported in Table 4. The barrier for the interconversion of the two S_4 structures in the gas phase is 105 cm^{-1}. This is rather similar to the difference calculated between the S_4 and D_{2d} structures at the MP2/6-31G* level theory (112 cm^{-1}).

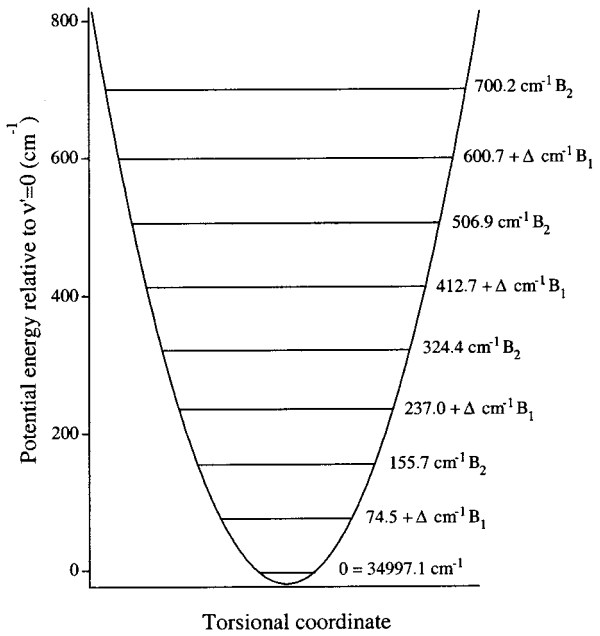

Figure 8. Energy levels and potential energy function of the ν_{20} torsional vibration in S_1 as deduced from the fluorescence excitation and emission spectra. Δ is the tunneling splitting of the first torsional quantum in the ground state (see Figure 7).

Within the employed computational approach, Franck−Condon intensities in the torsional progression in the excitation and fluorescence spectra can easily be calculated by overlapping the levels' wave functions. Figure 9 shows the first 800 cm^{-1} of the experimental and calculated fluorescence excitation spectra. Considering the simplicity of the model, the comparison is very satisfactory: the complicated pattern of progressions is

(19) Bell, R. P. *Proc. R. Soc. (London)* **1945**, *A183*, 328.
(20) Swalen J. D.; Ibers, J. A. *J. Chem. Phys.* **1972**, *56*, 4966.
(21) Hollas, J. M. *High-Resolution Spectroscopy*, 2nd ed.; John Wiley & Sons: Chichester, 1998.
(22) Leigh, D. A.; Troisi, A.; Zerbetto, F. *Angew. Chem., Int. Ed.* **2000**, *39*, 350.

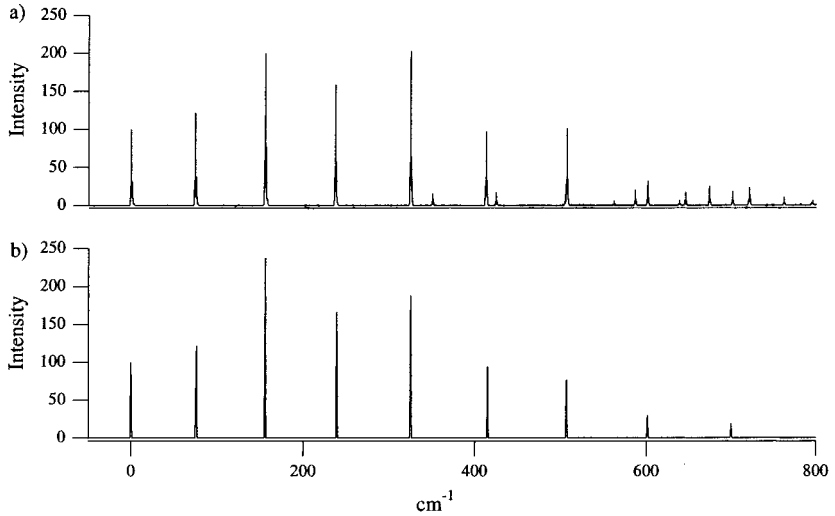

Figure 9. Comparison of experimental (a) and simulated (b) fluorescence excitation spectra of TTD. The simulated spectrum shows only the members of the ν_{20} progression.

Table 4. Parameters of the Potential Energy Curves ($V(x) = ax^2 + bx^4$) for the Torsional Potential of the Ground State and the First Excited State of TTD

electronic state	a (J m^{-2})	b (J m^{-4})	minimum (Å)	energy at minimum (cm^{-1})
S_0	−0.2429	7.044×10^{18}	±1.31	−105
S_1	0.2695	4.870×10^{18}	0	0

very well reproduced, and only the intensities of the third and seventh bands deviate more than 10% from the experimental values. It should be noticed that in the simulated spectra only the members of the progression based on the 0−0 transition are shown, while in the experiments other transitions involving the progression of the ν_{11} and ν_{10} totally symmetric modes are also present. A similar excellent agreement is found for the calculated and experimental single-level fluorescence spectra shown in Figure 10. Also in this case, the bands due to the progression of the totally symmetric mode are obviously not present in the simulations. Since the fitting was based only on the energy levels, the excellent agreement obtained for the intensities confirms a posteriori the validity of the potential selected. It should be emphasized that the complicated pattern observed experimentally is described with only four parameters.

The spectroscopic investigation of TTD and the simulations of excitation and emission spectra have unambiguously shown that the static symmetry of the molecule in its electronic ground state, i.e., that of the geometry of lowest energy, is not D_{2d} but is lowered to S_4. At the same time, these studies have demonstrated that upon excitation to the lowest excited singlet state the molecule recovers the high symmetry originally assumed for the ground state. These conclusions immediately give rise to two questions: (i) How can one explain the presence of the double minimum in the ground state of the gas-phase and its absence in the first electronically excited state? (ii) How can one reconcile the results obtained with nuclear magnetic resonance spectroscopy[10] and X-ray diffraction techniques[11] with those obtained here?

To start with the second question: For the NMR experiments one needs to consider whether tunneling between the two S_4 conformation is rapid on the NMR time scale. The tunneling rate constant for the ith torsional level can be estimated as[23] $k_i = 2\Delta\epsilon_i/h$, where $\Delta\epsilon_i$ is the tunneling splitting and h Planck's constant. At low temperatures, where only the lowest vibrational level is populated, the splitting of 1.4 cm^{-1} gives a rate constant of 8.4×10^{10} s^{-1}, which effectively averages out the motion on the NMR time scale. Higher temperatures populate more levels and give rise to even higher rates. The NMR measurements in chloroform are thus compatible with the two rapidly exchanging S_4 conformations observed in the gas phase.

For the X-ray diffraction results, one needs to consider the effect of the very low energy barrier on the probability distribution of the atoms. The effective displacement from D_{2d} geometry at room temperature can be estimated for the normal modes and the double-minimum displacement separately. Each motion has a probability, which is a function of the position in space, $P(r)$, and the temperature, that is given by

$$P(r) = \frac{\sum_n \chi_n^*(r)\chi_n(r)\, e^{-E_n/kT}}{\sum_n e^{-E_n/kT}}$$

where T is the temperature, χ the wave functions, and the other symbols are the usual constants. This equation can be used to generate the distribution of probability for the position in space of the atoms of TTD. Notice that while the vibrational coordinates are orthogonal to one another, they share the three-dimensional space. Figure 11 shows the probability distribution at room temperature along an idealized one-dimensional coordinate, the one associated with all the other normal modes, and their convolution. The distribution of probability is nearly the same over the entire coordinate and makes it plausible that even an X-ray investigation would lead to the conclusion that the molecule has D_{2d} symmetry in the crystal. Interestingly, doubling the energy barrier to 200 cm^{-1}, or doubling the distance between the two minima, yields two discernible maxima in the probability distribution.

(23) Deycard, S.; Lusztyk, J.; Ingold, K. U.; Zerbetto, F.; Zgierski, M. Z.; Siebrand, W. *J. Am. Chem. Soc.* **1988**, *110*, 6721. Zerbetto, F.; Zgierski, M. Z.; Siebrand, W. *J. Am. Chem. Soc.* **1989**, *111*, 2799. Deycard, S.; Lusztyk, J.; Ingold, K. U.; Zerbetto, F.; Zgierski, M. Z.; Siebrand, W. *J. Am. Chem. Soc.* **1990**, *112*, 4284.

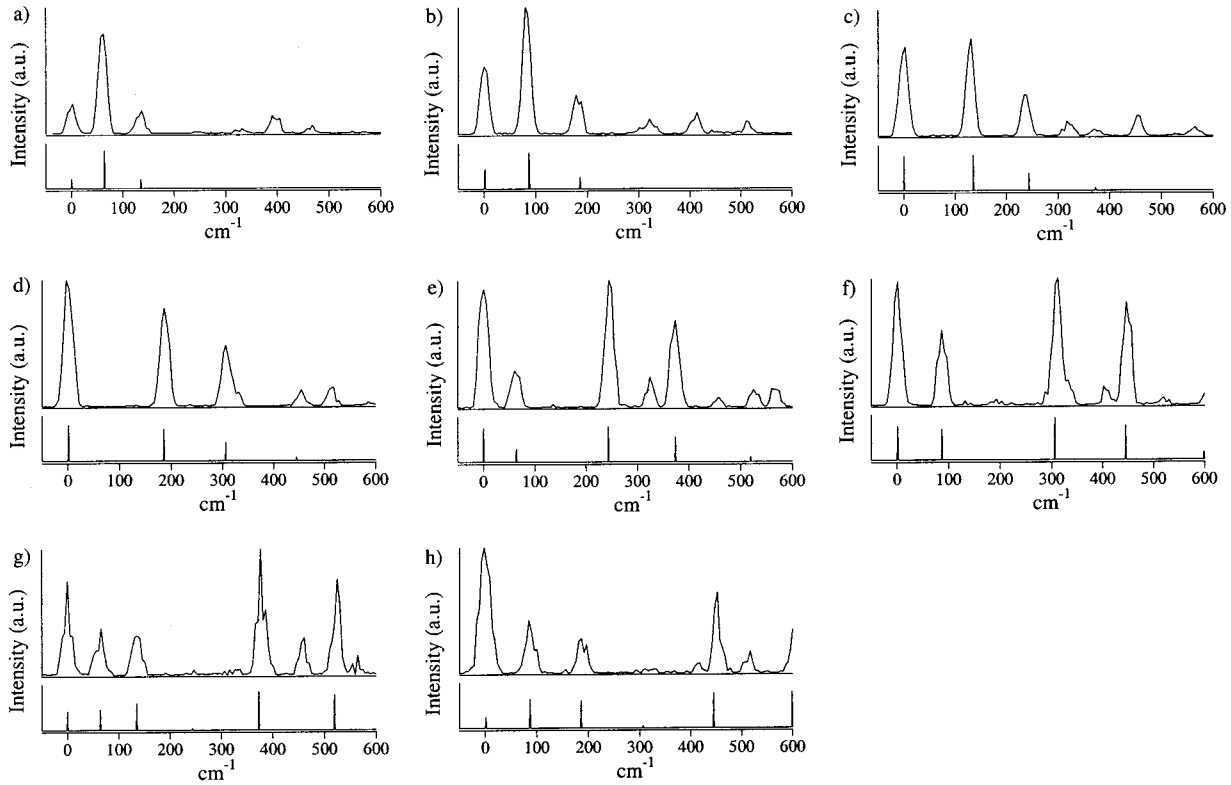

Figure 10. Comparison of experimental and simulated single-level fluorescence spectra of TTD. Excitation occurs in (a) via the 0−0 transition, in (b)−(h) via the bands 74.5 cm^{-1} (b), 155.7 cm^{-1} (c), 237.0 cm^{-1} (d), 324.4 cm^{-1} (e), 412.7 cm^{-1} (f), 506.9 cm^{-1} (g), 600.7 cm^{-1} (h) displaced from the 0−0 transition. The simulated spectrum shows only the members of the ν_{20} progression.

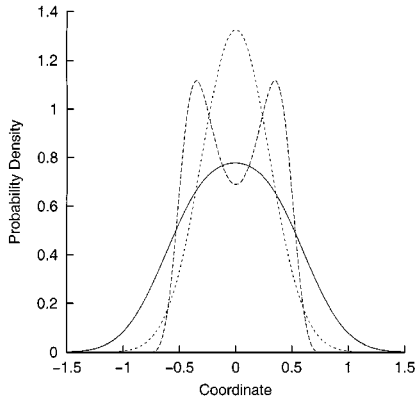

Figure 11. Probability distribution of the atoms positions along the S_4 interconversion potential at room temperature: solid line is the overall probability, dashed line is the double minimum potential probability, dotted line is the probability for all the other modes.

The observation that the Raman spectrum measured in the present study in the solid state seems to display activity in the ν_{20} (a_2) mode, which would nominally be forbidden, allows the conclusion that the gas-phase double-minimum potential of TTD does not change in the condensed phases. However, the NMR and X-ray results show that full detection of the S_4 minima is not easily accomplished.

The preference of TTD for the lower-symmetry S_4 structure in the electronic ground state may be attributed to a number of stereoelectronic effects. In particular, reduced repulsion between the lone pair orbitals and increased hyperconjugation between the lone pairs and the CH-σ^* orbitals are likely to be important. In contrast to TTD, the structurally related DABCO does not twist its N−C−C−N fragments to distort from the high D_{3d} symmetry,[24] although the frequency of the symmetry-breaking vibration is low (58 cm^{-1}).[25] One might speculate that the angle strain induced by the distortion of the smaller six-membered rings of DABCO is responsible for the difference.

The final issue to address is the difference between the conformations of the ground state and the first electronically excited state. For this purpose CIS calculations have been performed on the first excited singlet state. The Chelp scheme[26]—in which the atomic charges are fit to an electrostatic potential at selected points—showed subsequently that in the D_{2d} conformation of S_1, the nitrogen atoms have a negative charge smaller by 0.19 au than in S_0. Similarly, one set of carbon atoms is more positive by 0.33 au, while the other is less negative by 0.12 au. The two sets of hydrogen atoms are more negative by 0.14 and 0.06 au, respectively. Simple electrostatic calculations carried out with these charges show that the reduced interaction between the nitrogen atoms is ultimately responsible for the higher symmetry in the excited state. In S_1, the interatomic Coulomb interaction is lowered by 910 cm^{-1}. The result is that the other weakly binding interactions are not overcome by the electrostatic repulsion, and the excited state does not distort.

The present study has thus convincingly shown that—at odds with previous expectations and conclusions—the conformation of lowest energy of TTD in its electronic ground state does not possess D_{2d} symmetry but is of S_4 symmetry. How, then, about the ground state of the radical cation? As mentioned in the

(24) Yokozeki, A.; Kuchitzu, K. *Bull. Chem. Soc. Jpn.* **1971**, *44*, 72.
(25) Quesada, M. A.; Wang, Z.-W.; Parker, D. H. *J. Phys. Chem.* **1986**, *90*, 219.
(26) Breneman, C. M.; Wiberg, K. B. *J. Comput. Chem.* **1990**, *11*, 361.

Introduction, initial ESR experiments[12] gave puzzling results that could not be put into agreement with a D_{2d} or with a C_{2v} (or S_4) geometry. Our previous studies[3] on 1-azabicyclo[2.2.2]-octane, 1-azaadamantane, and 1,4-diazabicyclo[2.2.2]octane have demonstrated that the geometry and the spectroscopic properties of the molecule in the ground state of its radical cation can be determined excellently from high-resolution gas-phase spectroscopic studies of the same properties in the lower excited (Rydberg) singlet states. In the present case, this strategy leads to the inevitable conclusion that $TTD^{\bullet+}$ in its electronic ground state is of the same symmetry as in S_1, i.e., of D_{2d} symmetry! In an accompanying paper,[27] which describes a new study of the radical cation of TTD with magnetic resonance, optical spectroscopic, and computational techniques, it is shown that this conclusion is indeed correct.

IV. Conclusions

High-resolution gas-phase spectroscopy employing fluorescence excitation and single-level dispersed emission spectroscopy, in combination with ab initio calculations, has enabled us to unravel, at first sight, conflicting information on the geometry and photophysical properties of TTD and its radical cation offered by various experimental and theoretical techniques. A complex but coherent picture is offered by these studies, in which the cage structure drives the electronic and vibrational properties governing the electronic states and the atomic interactions, which ultimately bear on the molecular conformation and its dynamics. As a result, the molecule has a *static* S_4 symmetry in its electronic ground state that turns into a *dynamic* D_{2d} symmetry by the effects of tunneling through a barrier of ~0.3 kcal/mol. Interestingly, it has been found that DFT calculations with the hybrid density functional B3LYP, which was previously employed successfully for similar molecules, are not able to predict this behavior correctly. Only at the MP2 level, correlation is apparently incorporated correctly, because with this computational approach a quantitative agreement with experimental results is obtained. For the first excited singlet state, a Rydberg state of 3s character, it has been concluded that a static D_{2d} symmetry is recovered. This result concurrently implies that also the ground state of the radical cation most likely is of D_{2d} symmetry.

Acknowledgment. We thank Prof. S. F. Nelsen for bringing the "TTD problem" to our attention and providing us with a sample, Prof. J. W. Hofstraat and Dr. B. Rossenaar (Akzo Nobel, Arnhem) for measuring the FT-Raman spectrum of TTD, Ing. D. Beblaar for valuable experimental assistance, and Prof. C. A. de Lange for use of equipment. This research was supported (in part) by the Council for Chemical Sciences of The Netherlands Organization for Scientific Research (CW-NWO).

JA016971B

(27) Zwier, J. M.; Brouwer, A. M.; Keszthelyi, T.; Balakrishnan, G.; Offersgaard, J. F.; Wilbrandt, R.; Barbosa, F.; Buser, U.; Amaudrut, J.; Gescheidt, G.; Nelsen, S. F.; Little, C. D. *J. Am. Chem. Soc.* **2002**, *124*, 159 (following paper in this issue).